

Original Research

Are we focusing on the right parameters? Insights from Global Sensitivity Analysis of a Functional-Structural Plant Model

Rik J. L. Rutjens^{1,*}, Jochem B. Evers², Leah R. Band^{1,3}, Matthew D. Jones⁴
and Markus R. Owen¹

¹School of Mathematical Sciences, University of Nottingham, University Park, NG7 2RD, Nottingham, UK

²Centre for Crop Systems Analysis, Wageningen University & Research, Bornsesteeg 48, 6708PE, Wageningen, The Netherlands

³Division of Plant and Crop Sciences, School of Biosciences, University of Nottingham, Sutton Bonington Campus, LE12 5RD, Loughborough, UK

⁴School of Geography, University of Nottingham, University Park, NG7 2RD, Nottingham, UK

*Corresponding author's e-mail address: rik.rutjens@rmit.edu.au

Handling Editor: Tsu-Wei Chen

Abstract. Performing global sensitivity analysis on functional-structural plant models (FSP models) can greatly benefit both model development and analysis by identifying the relevance of parameters for specific model outputs. Setting unimportant parameters to a fixed value decreases dimensionality of the typically large model parameter space. Efforts can then be concentrated on accurately estimating the most important input parameters. In this work, we apply the Elementary Effects method for dimensional models with arbitrary input types, adapting the method to models with inherent randomness. Our FSP model simulated a maize stand for 160 days of growth, considering three outputs, namely yield, peak biomass and peak leaf area index (LAI). Of 52 input parameters, 12 were identified as important for yield and peak biomass and 14 for LAI. Over 70 % of parameters were deemed unimportant for the outputs under consideration, including most parameters relating to crop architecture. Parameters governing shade avoidance response and leaf appearance rate (phyllonchro) were also unimportant; variations in these physiological and developmental parameters do lead to visible changes in plant architecture but not to significant changes in yield, biomass or LAI. Some inputs identified as unimportant due to their low sensitivity index have a relatively high standard deviation of effects, with high fluctuations around a low mean, which could indicate non-linearity or interaction effects. Consequently, parameters with low sensitivity index but high standard deviation should be investigated further. Our study demonstrates that global sensitivity analysis can reveal which parameter values have the most influence on key outputs, predicting specific parameter estimates that need to be carefully characterized.

KEYWORDS: Elementary effects; global sensitivity analysis; functional-structural plant model; Morris method.

1. INTRODUCTION

Models in the biological and environmental sciences typically have many free parameters (Razavi and Gupta 2015; Qian and Mahdi 2020; Puy *et al.* 2021). This is, in particular, true for functional-structural plant models (FSP models) (Evers and Bastiaans 2016; Henke *et al.* 2016; Zhu *et al.* 2017) which simulate growth and development of plants in 3D as a function of environmental factors such as light, temperature and nutrition. Calibration of these parameters often requires empirical data, which can be costly or simply impossible to obtain (see Qian and Mahdi (2020) and the references therein). However, often only a small subset of input parameters in a system has a significant

influence on a specific system output (Box and Meyer 1986; Razavi *et al.* 2021). As such, it is beneficial for model development to identify unimportant parameters, so that they may be set to a fixed value and so that efforts can be concentrated on accurately estimating the most important input parameters. This can greatly decrease dimensionality of the model parameter space while increasing trust in the model. Sensitivity analysis (SA), the study of how variability in the model output can be attributed to the variability in the model inputs, is a common tool for identifying (un)important input parameters.

Local sensitivity analysis techniques in the form of one-at-a-time (OAT) methods involve changing one parameter at a time

from a fixed base point and assessing the effect on the model output (Pianosi et al. 2016). This assessment may involve the use of (potentially discretized) derivatives or might simply involve visual inspection of the model outputs (Pianosi et al. 2016). Because of their simplicity and ease of implementation, these methods for local SA are commonly used, although local SA methods may only prove informative in very specific situations (e.g. inverse problems or approximating a model output in a small region of output space) (Saltelli and Annoni 2010). In general, local sensitivity analysis is not recommended for rigorous SA; global methods (GSA) should be used instead (Saltelli et al. 2008; Saltelli and Annoni 2010). Global sensitivity analysis methods address the limitations of local OAT techniques by considering the entire space of variability of the input parameters (Pianosi et al. 2016). A variety of approaches have been proposed for GSA (Fig. 3 in Pianosi et al. (2016) compares some of them), based on different philosophies and theories, leading to different notions of (global) sensitivity (Saltelli and Tarantola 2002; Razavi and Gupta 2015). While there are certainly examples of GSA in FSP modelling (Cournède et al. 2013; Mathieu et al. 2016; Streit et al. 2016; Sainte-Marie and Cournède 2019; Zhu et al. 2021), in other cases, SA has not yet been applied or analyses may consist solely of OAT or visual inspection of model outputs (Vos et al. 2007; Buck-Sorlin et al. 2011; Henke et al. 2016; Coussement et al. 2018; de Vries et al. 2020; Bailey and Kent 2021; Gauthier et al. 2021; Pao et al. 2021; van der Meer et al. 2021; Pao et al. 2021). This does not invalidate the modelling exercise, but does highlight that GSA is not yet typically incorporated as standard into the study of FSP models.

The objective of this study is to show the benefit of performing GSA in FSP models. In particular, we apply the elementary effects method (EE) (also known as Morris' method Morris (1991)) to an FSP model simulating maize to identify (un)important parameters, assess the potential for model improvement and simplification and identify which biological processes might be more or less important for three model outputs, namely leaf area index (LAI), aboveground biomass and yield. The elementary effects method was chosen because it is a simple and commonly used GSA method designed to screen for (un)important parameters and is capable of identifying non-linear or interaction effects. EE has been used to analyse crop models (e.g. Richter et al. 2010; Vanuytrecht et al. 2014; Casadebaig et al. 2016; Caubel et al. 2017; Silvestro et al. 2017), but applications to FSP models are rare. We use the recently published version with scaled effects here, as described in Rutjens et al. (2023), which makes the method applicable to dimensional models with inputs of arbitrary range and inputs of integer or Boolean type and prevents erroneous rankings. Several other common approaches, including those that take the dependency structure of the inputs into account (Owen 2014) are described in Saltelli et al. (2008), Razavi and Gupta (2015), Qian and Mahdi (2020) and the references therein.

2. ELEMENTARY EFFECTS METHOD

The idea behind EE is to characterize the space of model outputs by a relatively low number of strategically placed simulation

points. From these simulation points, we are then able to calculate finite differences (called *elementary effects*) as measures of how the output changes when one input changes. Finally, by aggregating these effects for each combination of input and output in a certain way, we obtain measures of (global) sensitivity of the outputs for the inputs. In this work, we define the sensitivity of output Y_j to input parameter X_i to be the relative contribution of the variability in the input parameter to the variability of the output. The asserted (finite) range of an input parameter is used here as input variability and variance in the output as output variability (which is a common choice (Razavi and Gupta 2015)), but other notions of input and output variability can in principle be used as well, such as mean, standard deviation or interquartile range. This section follows (Rutjens et al. 2023). We refer to that work and the references therein for further detail.

2.1. Definition of elementary effects

Let $X_i, i = 1, \dots, k$ be dimensional input parameters with units $[X_i]$, taking values in $[\min_i, \max_i]$ uniformly. If the parameter can only take integer values, it takes values in the set $\{\min_i, \min_i + 1, \dots, \max_i\}$. The same holds for Boolean parameters, but then $\min_i = 0$ and $\max_i = 1$, where 0 encodes false and 1 stands for true. x_i denotes the dimensionless equivalent scaled to the unit interval, that is,

$$x_i = \frac{X_i - \min_i}{\max_i - \min_i}, \quad (1)$$

henceforth referred to as *scaled dimensionless* parameters. The dimensional outputs of interest are denoted by $Y_j, j = 1, \dots, q$ with corresponding unit $[Y_j]$. An *elementary effect* for output Y_j and input parameter X_i at base point $\mathbf{X}^n = (X_1^n, \dots, X_k^n)$ is then defined as the finite difference

$$EE_{ij}^n = \frac{Y_j(X_1^n, \dots, X_{i-1}^n, X_i^n + \Delta_i^n, X_{i+1}^n, \dots, X_k^n) - Y_j(\mathbf{X}^n)}{\Delta_i^n}. \quad (2)$$

Here, the superscript n is simply an index to distinguish different \mathbf{X} , to emphasize that the EE can be calculated at numerous points in the parameter space. Δ_i^n represents the step in the actual parameter space, which depends on the scaled dimensionless step $\delta_i^n \in [0, 1]$ in the following way:

$$\Delta_i^n = \delta_i^n (\max_i - \min_i). \quad (3)$$

The value of δ_i^n follows from the chosen trajectory generation method and is calculated a posteriori (see Section 2.2 and Supporting Information—Supplementary Material S1). The effect EE_{ij}^n given by Equation (2) is dimensional with units $[EE_{ij}^n] = [Y_j]/[X_i]$.

While here we assume uniformly distributed inputs, this can be relaxed to include arbitrary distributions. Scaling the sampled parameter values from $[0, 1]$ to the actual interval should then be done using the corresponding inverse cumulative density function (CDF).

2.2. Trajectory generation

It is generally not feasible (nor desirable) to calculate every possible effect; even with discrete-valued inputs, the number of

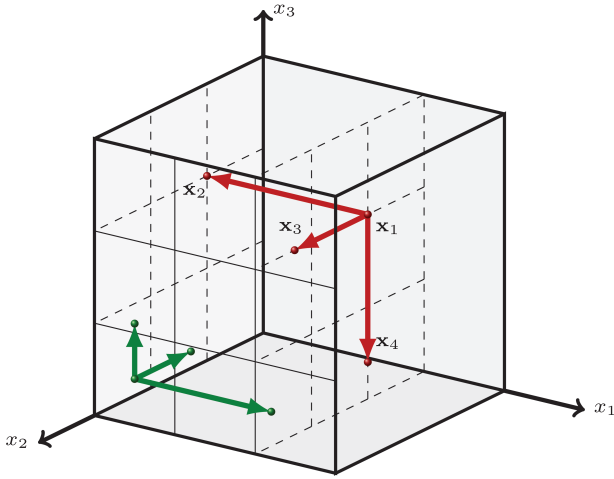


Figure 1. Radial design sample in the unit cube with $k = 3$ parameters and $r = 2$ trajectories. \mathbf{x}_1 is a base point, \mathbf{x}_2 , \mathbf{x}_3 and \mathbf{x}_4 are perturbed points.

required simulations quickly becomes prohibitive. Instead, the goal is to generate a small set of $Q = r(k + 1)$ simulation points, typically $Q \sim 1000$, which still provides good coverage of the parameter space. Here, r is the number of effects for each input. The sensitivities are then characterized by some aggregation measure and standard deviation over r effects. In this work, the Q simulation points are clustered into r star-shaped trajectories (Fig. 1; also called a radial design), where the base point (\mathbf{x}_1 in Fig. 1) is used repeatedly in combination with the perturbed points ($\mathbf{x}_2 - \mathbf{x}_4$) for the calculation of the elementary effects. To ensure a uniform distribution of the r base points in the parameter space, a quasi-random (QR) or low-discrepancy sequence is typically used (Morokoff and Cafisch 1994; Hickernell 2000; Saltelli et al. 2010; Campolongo et al. 2011). QR sequences are designed to produce point sets that cover a space both efficiently (i.e. with a low number of points) and evenly (i.e. approximating a uniform distribution). In this work, we consider the recently presented R_d sequence (Roberts 2021), which has been shown to perform well in EE (Rutjens et al. 2023). The QR sequence is used to generate a set of r base points (gathered in a $r \times k$ matrix A) and a set of r perturbation vectors ($r \times k$ matrix B). Each pair of base point and perturbation vector then leads to a star-shaped trajectory in parameter space [see Supporting Information—Supplementary Material S1].

For Boolean or integer input parameters, an adjustment is required to avoid non-integer/Boolean parameter values in the actual parameter space for these parameters (Rutjens et al. 2023). We pin the base point coordinates corresponding to integer/Boolean inputs to a discrete value and then use a fixed step size. In other words, given a base coordinate x_i in $[0, 1]$ generated by a QR sequence, we transform the coordinate to a discrete value \tilde{x}_i by:

$$\tilde{x}_i = \begin{cases} 1 & \text{if } x_i = 1; \\ \lfloor p_i x_i \rfloor / p_i & \text{else,} \end{cases} \quad (4)$$

where p_i (the number of discrete values input i can take) satisfies

$$\max_i - \min_i = m(p_i - 1), \quad (5)$$

for some $m \in \mathbb{N}$. While \tilde{x}_i is not necessarily integer/Boolean, the coordinate in the actual parameter space is given by:

$$\begin{aligned} X_i &= (\max_i - \min_i)\tilde{x}_i + \min_i \\ &= m(p_i - 1)\tilde{x}_i + \min_i \\ &= \begin{cases} \max_i & \text{if } x_i = 1; \\ m\lfloor p_i x_i \rfloor + \min_i & \text{else} \end{cases} \end{aligned}$$

for some $m \in \mathbb{N}$, which is an integer/Boolean. Subsequently, the perturbed point is found by stepping with fixed step size

$$|\Delta_i| = \frac{n(\max_i - \min_i)}{p_i - 1}, \quad (6)$$

where $n \in \{1, 2, \dots, p_i - 1\}$ is to be chosen, such that the perturbed point still lies in the parameter space. Whenever possible, p_i should be chosen to be even and $n = p_i/2$ to ensure equal sampling probabilities (Morris 1991).

2.3. Scaled effects and sensitivity measure

Scaling effects in the input-direction and using a dimensionless sensitivity measure are essential when input parameters are dimensional and take values on non-unit intervals, in order to prevent erroneous rankings and to obtain results consistent with the notion of global sensitivity (Rutjens et al. 2023). This is not standard practice yet (see, e.g. Menberg et al. 2016; Pao et al. 2021; Uys et al. 2021) and not all third-party GSA implementations include both of these additional steps (in particular the use of a dimensionless sensitivity measure) Iooss et al. (2021); Pianosi et al. (2015). Following Rutjens et al. (2023), we scale effects by the input range

$$c_{x_i} = \max_i - \min_i. \quad (7)$$

The scaled effect $EE_{ij}^n \cdot c_{x_i}$ has units $[Y_j]$. Subsequently, we define the dimensionless normalized sensitivity measure

$$S_{\chi}(i, j) = \frac{\chi_{ij} c_{x_i}}{\sum_{l=1}^k \chi_{lj} c_{x_l}}, \quad (8)$$

where χ_{ij} is the median of the absolute effects $\{|EE_{ij}^n|\}_{n=1, \dots, r}$. The $S_{\chi}(i, j)$ take values in $[0, 1]$ and sum to unity (over i for fixed output j). This allows for a standardized way of identifying the (un)important parameters (Wu 2020). For a given output Y_j , the $S_{\chi}(i, j)$'s are sorted in ascending order leading to a sequence

$$S_{\chi}(i_1, j) < S_{\chi}(i_2, j) < \dots < S_{\chi}(i_k, j). \quad (9)$$

The q unimportant parameters are then those for which

$$\sum_{m=1}^q S_{\chi}(i_m, j) < \frac{h}{100}, \quad \sum_{m=1}^{q+1} S_{\chi}(i_m, j) \geq \frac{h}{100}, \quad (10)$$

where h is a predefined percentage (10% in Wu (2020), although they note a low h -value may lead to incorrectly identifying parameters as important). Important parameters for a given output are those with a value of the sensitivity index S_{χ} above a

pre-determined threshold S_{0j} . This quantity may be a function of the $S_{\chi}(i, j)$'s, making it a function of the threshold h through Equation (10) (essentially $q = q(h)$); here

$$S_{0j}(h) = \hat{\mu}_{0j} + 3\hat{\sigma}_{0j} \quad (11)$$

is used (as in Wu (2020) and Rutjens et al. (2023)), where $\hat{\mu}_{0j}$ and $\hat{\sigma}_{0j}$ are the sample mean and standard deviation of the $S_{\chi}(i, j)$'s corresponding to unimportant variables, that is,

$$\hat{\mu}_{0j} = \frac{1}{q} \sum_{m=1}^q S_{\chi}(i_m, j), \quad (12)$$

$$\hat{\sigma}_{0j} = \sqrt{\frac{1}{q-1} \sum_{m=1}^q (S_{\chi}(i_m, j) - \hat{\mu}_{0j})^2}. \quad (13)$$

Finally, to gain insight into the non-linear response of outputs to inputs and detect potential interaction effects, we consider the relative standard deviation (RSD) defined by

$$\text{RSD}_{ij} = \frac{\sigma_{ij}}{\mu_{ij}^*} \times 100\%, \quad (14)$$

where σ_{ij} is the standard deviation of the (non-absolute) effects $\{EE_{ij}^n\}_{n=1, \dots, r}$ and μ_{ij}^* is the mean of the absolute effects $\{|\EE_{ij}^n|\}_{n=1, \dots, r}$. In other works (Ruano et al. 2012; Yang and Becerik-Gerber 2015; Menberg et al. 2016), ratios of μ^* and σ are used to classify levels of non-linearity, interaction effects or general importance, but in this work, RSD is purely used as a tool to inform which parameters might deserve a more detailed follow-up (i.e. those with a small sensitivity index S_{χ} but a high RSD).

3. MODEL DESCRIPTION

The model considered here is a general modular FSP model using the modelling platform GroIMP (Hemmerling et al. 2008). It simulates aboveground plant growth and architectural development, driven by competition between plants for light and nutrients. It is an evolution of the model presented in Evers and Bastiaans (2016).

In this study, we simulate maize plants at a daily time step based on the principles of assimilate supply and demand. Plant organs serve either as a pure sink for assimilates (the generative organs and the roots) or both as a source and a sink depending on their age and surface area (the leaves and the stem segments).

3.1. Environment

To accurately represent a realistic light field, a mix of direct and diffuse light sources are placed in the scene. Seventy-two diffuse light sources are configured in 6 rings at different heights and 24 direct light sources describe an arc in the sky to emulate the sun's path (Evers and Bastiaans 2016). The angle and orientation of the arc depend on the day of the year and latitude; the power of the light sources depends on the day of the year, the location in the sky, latitude and transmissivity. The relative contribution of the diffuse and direct light sources is constant over a simulation, with the fraction of diffuse light of the

total incoming radiation set to 0.8. Further details of the diffuse/direct radiation calculation can be found in Goudriaan and Van Laar (1994), Spitters et al. (1986) and Spitters (1986). At each time step, rays of photosynthetically active radiation (PAR) cast by the light sources are absorbed, reflected or transmitted by leaves and stems according to organ-independent optical coefficients, using the stochastic ray tracer capabilities of GroIMP (Hemmerling et al. 2008).

The average daily temperature follows a sinusoidal pattern over the year, reaching its minimum value around day 20, mean at day 111, and its maximum around day 202 (Evers and Bastiaans 2016). It is characterised by a mean value (tav_a) and the amplitude of the deviation around that mean (tav_b). Other atmospheric parameters such as CO₂ level, vapour pressure deficit and O₂ level are kept constant throughout a simulation.

3.2. Physiology

At the organ level, the absorbed PAR is used to calculate the photosynthesis rate as a function of organ nitrogen level (Evers and Bastiaans 2016). Assimilated CO₂ is converted into growth substrates, and maintenance costs are deducted. This leads to a daily pool of substrates available for organ growth.

Photosynthesis is described by a C4-equivalent of the Farquhar-von Caemmerer-Berry (FvCB) model as in Yin and Struik (2009). The FvCB model implemented here predicts the net photosynthesis rate as the minimum of the Rubisco-limited and the electron transport-limited rates of CO₂ assimilation. The FvCB model is the standard in relating photosynthetic carbon assimilation to the concentration of intercellular CO₂ and absorbed photosynthetically active radiation (Dubois et al. 2007). While parameter values for the original C3 model have been calibrated fairly precisely, there are a number of parameters in the C4-equivalent with more uncertainty (Yin and Struik 2009). We take nine of the FvCB parameters into account in the sensitivity analysis (Table 1, parameters 35–43).

Potential organ growth rate is defined as the organ demand for growth substrates (its sink strength), implemented using the first derivative of a beta growth function (Yin et al. 2003; Evers and Bastiaans 2016). To determine actual growth rate, the relative sink strength concept is used (Heuvelink 1996), in which the sink strength of an organ is expressed as a fraction of total plant sink strength. Depending on substrate availability and relative sink strength, organs grow at or below their potential rate. Any excess growth substrates stored from all organs are made available for growth in the next time step.

Finally, organ size is updated based on the substrates received by each organ, using parameters for leaf mass per unit of leaf area (LMA) for the leaves, and specific internode length (SIL) for the internodes. Specifically for internodes, additional extension due to shade avoidance (Huber et al. 2021) is implemented by making SIL dependent on the level of competition experienced by the plant (Evers and Bastiaans 2016).

3.3. Plant development

Plant development is temperature driven, with a daily thermal time increment depending on the average daily temperature (see Section 3.1) and the species base temperature. We suppose

plants germinate on the same day. Subsequent leaves are initiated and appear at constant thermal time intervals (plastochron and phyllochron, respectively). The total number of phytomers produced during a plant's lifespan is taken as constant and equal for all plants. If a leaf reaches a certain age or receives less light over a day than a given threshold, it will be shed.

3.4. Plant architecture

To mimic maize architecture, the first given number of internodes do not elongate (parameter 18: nrShortInternodes), resulting in the corresponding leaves emerging near the soil level. Leaves are represented by narrow oblong surfaces (see Evers and Bastiaans (2016) and Figs. 7 and 8). Consecutive leaves appear along the stem at a constant phyllotactic angle. The root system architecture is not explicitly modelled.

4. SIMULATIONS AND ANALYSIS

For each of the selected simulation points (as described in Section 2), we simulate a field of 100 maize plants until harvest at day 159. The field is cloned 10 times in each direction to eliminate border effects. Three outputs are considered: yield at the final simulation day (grain biomass per m²), peak above ground biomass and peak LAI (in m² of leaf area per m² of ground area).

4.1. Model parameters

Fifty-two parameters are taken into account in this analysis. Their input ranges and brief descriptions are included in Table 1. Inputs are grouped into four categories, namely architectural, developmental, environmental and physiological (Table 1).

For each parameter, 40 effects (hence 40 trajectories) are considered in a radial design as described in Supporting Information—Supplementary Material S1, leading to a total of $40 \times (52 + 1) = 2120$ simulations per replicate (Section 4.2). For determining what parameters are (un)important, an h -level (Equation (10)) of 30 % is used.

Furthermore, a number of model parameters are fixed throughout the analysis as they have known and fixed values (e.g. latitude) or concern management practices (e.g. row distance). Their values and descriptions are listed in Table 2 in Supporting Information—Supplementary Material S2.

4.2. Inherent model randomness

EE is designed for deterministic models. Our model, however, contains inherent randomness, not caused by the input parameters, but, for example, by small random perturbations in internode orientation or leaf angle (to capture the natural variation of a species population) or by inherent randomness in the light sub-model. To address this, we repeat each of the simulations three times, and average the outputs of the three replicates at each simulation point. We then calculate effects and sensitivity indices of these averaged values. Since the relative standard deviation (RSD) of the output values of the different replicates at each simulation point—the standard deviation of three replicates divided by the mean—is low (Fig. 2), we argue three replicates is sufficient in this case.

4.3. Effect outliers

Because we use a quasi-random (QR) sequence Roberts (2021) to generate the simulation points, in a small number of cases the distance from base point to perturbed point is relatively very small (Fig. 3). This is not a problem if the model is deterministic, but since our model contains inherent randomness it can cause effect outliers, which could cause changes in the sensitivity indices. This can be seen as follows. We split the output Y in a deterministic part (i.e. the value if the model was deterministic) and a random part, which leads to the (unscaled) effect for input x_i and trajectory $n = 1, \dots, r$ given by:

$$EE_i^n = \frac{EE_{\text{det},i}^n}{\delta_i^n} + \frac{EE_{\text{rnd},i}^n}{\delta_i^n}. \quad (15)$$

A problem arises if there are a few n for which $|\delta_i^n| \ll 1$. The deterministic part $EE_{\text{det},i}^n/\delta_i^n$ should be the same order of magnitude for all n , but for the n with a very small (relative) step size the stochastic part $EE_{\text{rnd},i}^n/\delta_i^n$ may blow up and become dominant (relative to the other n with larger step sizes).

In preliminary experiments (not shown here), we found up to a thousandfold increase in the elementary effect compared to the mean for that parameter. To remedy this issue, we remove effect outliers. Specifically, assuming coordinates generated by a QR sequence are identical and independent uniformly distributed (so $x_i^n \sim \mathcal{U}([0, 1])$), the scaled dimensionless step size $|\delta_i^n|$ follows a triangle distribution with CDF $F(|\delta_i^n|) = 2|\delta_i^n| - |\delta_i^n|^2$ for $0 \leq |\delta_i^n| \leq 1$.

Outliers are then those effects for which the step size is an extreme value of this distribution, here defined as those for which $F(|\delta_i^n|) < 0.005$. It follows that all effects for which $|\delta_i^n| < 1 - \sqrt{398/20} \approx 0.0025$ are classified as outliers, and are thus removed from the analysis. In the results presented below, we removed 13 effects distributed over 12 inputs out of a total of $40 \cdot 52 = 2080$ elementary effects (Fig. 3).

5. RESULTS

With an unimportance threshold of $h=30\%$ (see Equation (10)) and the importance threshold given in Equation (11), 12 out of 52 parameters were classified as important (39 as unimportant) for the outputs yield and peak biomass, and 14 parameters were found to be important (37 unimportant) for peak LAI (Fig. 4 and Table 1). This leaves one parameter for each output that is neither unimportant nor important.

5.1. Important parameters

A number of parameters in the model currently take a value from the same input range for all species and/or organs, although it is known these are actually species- or even organ-specific. The fact that some of these—for example, growth respiration (parameter

Table 1. Parameters included in EE analysis, which belong to the indicated categories (A: architectural; D: developmental; E: environmental; P: physiological). All parameters are real numbers except 15, 18, 29 and 51 that are integers; in those cases, the description includes the number of levels p_i and step size $|\delta_i|$. Results from the GSA are shown in the right-most three columns, which indicate whether a parameter is found to be unimportant (x), important (number indicates rank, 1 being most important; top 5 in red) or neither (-) for three outputs. *: maximum plant biomass (before final simulation day); †: maximum leaf area index (before final simulation day).

Parameter	Category	Description	Units	min_i	max_i	Yield	Biomass*	LAI†	
1	Ca	E	Atmospheric CO ₂ level	ppm	300	600	x	x	x
2	VPD	E	Vapour pressure deficit	kPa	0.3	3	12	12	x
3	tav_a	E	For average temperature calculation	°C	9.095	12.305	4	4	14
4	tav_b	E	For average temperature calculation	°C	6.4175	8.6825	9	10	-
5	specificInternodeLength	A	Internode length per unit biomass (SIL)	m g ⁻¹	0.025	0.075	x	-	x
6	LMA	A	Leaf mass per unit area	mg cm ⁻²	4	7	7	6	1
7	lwRatio	A	Ratio of leaf blade length and width	-	9.18	11.22	x	x	x
8	maxWidth	A	Location where leaf width is maximal	-	0.6	0.7	x	x	x
9	shapeCoeff	A	Leaf shape coefficient	-	0.7	0.8	x	x	x
10	leafAngleLower	A	Insertion angle of leaves with rank equal to or below rankLower	°	40	75	x	x	x
11	leafAngleUpper	A	Insertion angle of leaves with rank above rankLower	°	20	60	x	x	11
12	leafCurve	A	Leaf curvature – angle between bottom and top of leaf blade	°	10	100	x	x	10
13	petioleFraction	A	Fraction of biomass partitioned to the petiole	-	0.0425	0.0575	x	x	x
14	specificPetioleLength	A	Petiole length per unit biomass	m g ⁻¹	2.125	2.875	x	x	x
15	rankLower	A	Number of lower phytomers that contain nrLeavesLower leaves; this partitions a plant in an lower and upper part with (potentially) different architectural properties Integer-valued, $p_i = 3, \delta_i = 1/2$	-	2	4	x	x	x
16	phyllotaxis	A	Angle between consecutive leaves along the stem	°	110	250	x	x	x
17	sheathscafeactor	A	Determines sheath width	-	20	40	x	x	x
18	nrShortInternodes	P	Number of bottom internodes that do not elongate Integer-valued, $p_i = 3, \delta_i = 1/2$	-	3	5	x	x	x
19	wmaxRoot	P	Maximal root system biomass (under ideal no-stress conditions)	mg	10 000	50 000	11	x	7
20	wmaxFlower	P	Maximal flower biomass	mg	200 000	400 000	8	x	x
21	wmaxInt	P	Maximal internode biomass	mg	3000	5000	x	x	x
22	wmaxLeaf	P	Maximal leaf biomass	mg	4000	6000	x	x	9
23	teRoot	P	Growth duration in thermal time of root system (no growth after this time)	°C day	1620	1980	x	x	x
24	teFlower	P	Growth duration in thermal time of flower	°C day	900	1100	x	x	x
25	teInt	P	Growth duration in thermal time of internode	°C day	450	550	x	x	x
26	teLeaf	P	Growth duration in thermal time of leaf	°C day	450	550	x	x	13
27	nitro	P	Nitrogen content of fully lit leaf	g m ⁻²	1.5	4	2	1	3
28	leafLife	P	Life span of leaf since appearance (expressed as number of times teLeaf)	-	2	4	x	x	x
29	varDelay	P	Max variation in germination delay Integer-valued, $p_i = 5, \delta_i = 2/4$	day	2	6	x	x	x
30	seedMass	P	Seed endosperm mass	mg	250	300	x	x	x

Table 1. Continued.

Parameter	Category	Description	Units	min _i	max _i	Yield	Biomass*	LAI†
31 SASmax	P	Shade avoidance syndrome amplitude factor ($c_{SAS} = 1 + (SASmax - 1) \exp(-SASk \cdot sr)$, where sr is the plant source/sink ratio)	–	10	30	x	x	x
32 SASk	P	Shade avoidance syndrome exponent factor	–	1	15	x	x	x
33 reflectancePAR	P	Reflectance of PAR by leaves and stem (fraction of incoming PAR)	–	0.07	0.15	x	x	x
34 transmittancePAR	P	Transmittance of PAR by leaves (fraction of incoming PAR)	–	0.04	0.15	x	x	x
35 k2ll_a	P	In calculation of conversion efficiency of incident light into electron transport at strictly limiting light	mol mol ⁻¹	0.0396	0.0484	x	x	x
36 k2ll_b	P		mol mol ⁻¹	0.1845	0.2255	x	11	x
37 Vcmax25_a	P	In calculation of maximum rate of Rubisco activity-limited carboxylation	μmol m ⁻² s ⁻¹	27.36	33.44	x	x	x
38 Vcmax25_b	P		μmol m ⁻² s ⁻¹	3.924	4.796	–	x	x
39 Jmax25_a	P	In calculation of maximum rate of e-transport under saturated light	μmol m ⁻² s ⁻¹	89.442	109.318	x	x	x
40 Jmax25_b	P		μmol m ⁻² s ⁻¹	5.175	6.325	x	x	x
41 Rd25	P	Day respiration (respiratory CO ₂ release other than by photorespiration)	μmol m ⁻² s ⁻¹	1.08	1.32	x	x	x
42 TPU25_a	P	For calculation of triose-phosphate utilization	μmol m ⁻² s ⁻¹	4.8303	5.9037	x	x	x
43 TPU25_b	P		μmol m ⁻² s ⁻¹	0.837	1.023	x	x	x
44 rg	P	Growth respiration	g g ⁻¹ day ⁻¹	0.255	0.345	10	9	12
45 kNkL	P	Ratio of leaf nitrogen and light extinction coefficients (k_N/k_L)	–	0.2	1	6	5	5
46 rm	P	Maintenance respiration	g g ⁻¹ day ⁻¹	0.01275	0.01725	x	–	x
47 fCO2	P	Conversion factor of CO ₂ to biomass	–	0.51	0.69	5	3	6
48 tb	D, P	Base temperature for thermal time calculation	°C	6	10	1	2	8
49 plastochronconst	D	Plastochron (thermal time between creation of two phytomers) is this constant ($\in [0, 1]$) times phyllochron, to ensure that plastochron is smaller than phyllochron	–	0.8	0.95	x	x	x
50 phyllochron	D	Thermal time between appearance of two leaves	°C day	25	35	x	x	x
51 finalPhytNum	D	Final number of main stem vegetative phytomers Integer-valued , $p_i = 6$, $ \delta_i = 3/5$	–	10	20	3	8	4
52 fallPAR	D	Light level below which leaf drops	μmol m ⁻² s ⁻¹	20	100	x	7	2

44: rg) or the conversion factor for CO₂ to biomass (parameter 47: fCO₂)—are identified as important suggests it might be appropriate to make these parameters species- or organ-dependent, for example, give them different input ranges for different species or organs. Likewise, average temperature parameters being identified as important for yield and peak biomass indicates that i) it is important to have accurate temperature data or

predictions; and ii) it might be beneficial to add a more detailed description (in time and/or space) of temperature.

This sensitivity analysis also suggests the description of some species-dependent parameters is too simplistic. As an example, leaf mass per unit area (parameter 6: LMA) is currently modelled as homogeneous in space and constant in time. In reality, this quantity is likely variable in both space and time (Zhou *et al.*

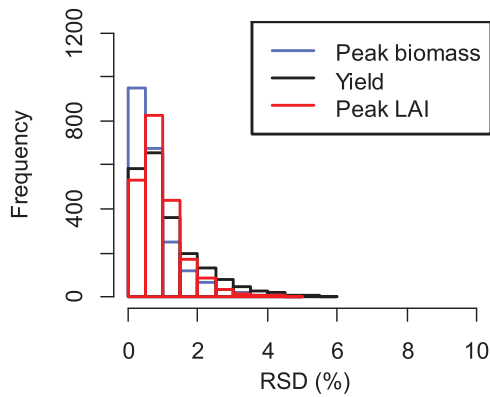


Figure 2. RSD, in %, Equation (14) over 3 replicates of outputs at each of the 2120 simulation points.

2020). This input is among the most important ones for all outputs, which implies it may be useful to include more detail in this aspect of the model.

Interestingly, some of the important parameters cannot generally be measured in an experimental setting, or at best can only be roughly estimated. Among these are theoretical maximum biomass of the root system, flower and leaf (parameters 19: wmaxRoot, 20: wmaxFlower and 22: wmaxLeaf).

5.2. Unimportant parameters

While two architectural parameters are identified as important for the output peak LAI (leaf curvature (parameter 12: leafCurve) and insertion angle of upper leaves (parameter 11: leafAngleUpper)), the vast majority are deemed unimportant for all outputs (Fig. 4). This suggests that, for the current maize model, parameters such as internode length per unit biomass (parameter 5: specificInternodeLength), petiole length per unit biomass (parameter 14: specificPetioleLength), angle between consecutive leaves (parameter 16: phyllotaxis) and a number of leaf shape parameters (parameters 7: lwRatio, 8: maxWidth, 9: shapeCoeff), which might be time-consuming or costly to measure, can be fixed or estimated more coarsely.

Furthermore, the parameters governing the strength of the shade avoidance syndrome (SAS; parameters 31 and 32) (in this case shade-induced internode extension) are identified as unimportant, even though the range for these parameters was quite wide. This does not mean that the SAS mechanism itself is irrelevant, as plant architecture changes significantly depending on the amount of competition Huber et al. (2021), but instead our analysis suggests that variation in the strength of the SAS response does not lead to significantly different LAI, yield or biomass.

Surprisingly, phyllochron (parameter 50) and plastochron (parameter 49) are also classified as unimportant. Simulations with phyllochron set to the minimum and maximum values of its input range show a noticeable effect on the architecture (Fig. 8), but, like SAS, our analysis suggests that this does not translate to a significant impact on field-level outputs yield, peak biomass or peak LAI (Fig. 6).

5.3. Relative standard deviation

A number of inputs have a low sensitivity index but high RSD Equation (14), such as PAR reflectance (parameter 33: reflectancePAR) and transmittance (parameter 34: transmittancePAR) by leaves and stem, and a photosynthesis parameter used in the calculation of the maximum rate of Rubisco activity-limited carboxylation (parameter 37: Vcmax25_a) (Fig. S6 in Supporting Information—Supplementary Material S4). While the mean response of an output to changes in such an input is low, there are high fluctuations around this mean, which would indicate non-linearity or interaction effects. This makes it unclear whether these parameters are actually unimportant. We found that there can be a variety of reasons for a high RSD (see Fig. S6 in Supporting Information—Supplementary Material S4). On one end of the spectrum are inputs with a single (absolute) effect that is much larger than the others, solely causing a high standard deviation of effects. This might indicate very local non-linearity or interaction effects, or suggest important parts of parameter space have not been sufficiently covered by the chosen number of trajectories. On the other end are the inputs for which effects are evenly distributed around the mean, indicating a more general non-linear trend or more global interaction effects. There does not seem to be a clear correlation between large effects and small step sizes for such effects (Fig. 3 and Supporting Information—Supplementary Fig. S6).

5.4. Illustrative (local) OAT simulations

We performed an illustrative (local) OAT study for three parameters that were identified as important (nitrogen content of fully lit leaf (parameter 27: nitro), maize base temperature (parameter 48: tb), conversion factor of CO₂ to biomass (parameter 47: fCO₂)) and three inputs found to be unimportant for all outputs (leaf shape coefficient (parameter 9: shapeCoeff), phyllochron (parameter 50: phyllochron), PAR reflectance by stem and leaves (parameter 33: reflectancePAR)) (Fig. 6). The baseline is taken to be the mean of each input's range, and the six inputs are then varied over their ranges uniformly. Consistent with the results from the GSA, the OAT method shows that the three important parameters have a significant effect on the outputs, while the unimportant parameters have negligible effects (Fig. 6). This is purely an illustrative example; OAT is not a replacement for rigorous GSA, and the output response could be different at another baseline in parameter space. Figures 7 and 8 show the effect on the plant architecture of varying leaf nitrogen content (parameter 27: nitro) and phyllochron (parameter 50: phyllochron), respectively.

5.5. Further observations

While maximum biomass is typically attained at the last simulation day, there is a large variation in the time when maximum LAI is achieved, as the precise pattern of leaf senescence hardly plays a role for biomass accumulation, while it does for LAI (Fig. 9). The simulation day at which maximum LAI is achieved approximately follows a normal distribution with mean 103 (days) and standard deviation 17.74 (days), noting that all the simulations where the maximum was at (or

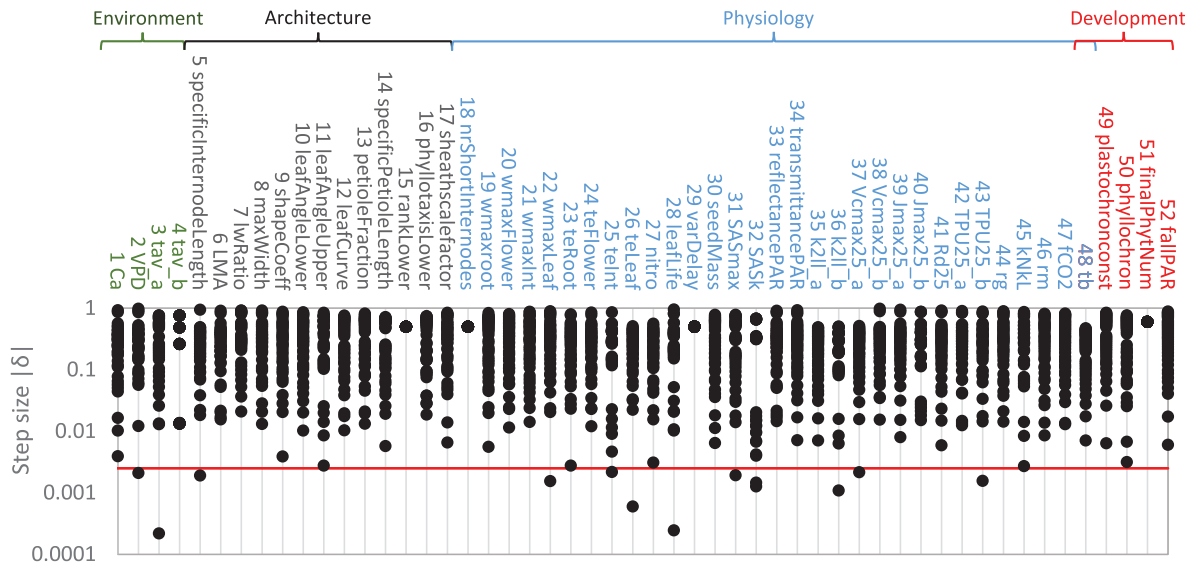


Figure 3. Scaled dimensionless step sizes ($|\delta_i^{\#}| \in [0, 1]$) for each input parameter, which follow from the chosen trajectory generation method (Section 2.2). Effects corresponding to step sizes smaller than the threshold (red line) are labelled as outliers and removed from the analysis. The threshold is described in Section 4.3. The label colours represent the parameter categories. Black: architectural; red: developmental; green: environmental; blue: physiological. See Table 1 for more information about the input parameters.

would be after) the final simulation day are grouped in the bin for day 159.

Plotting the sensitivity indices for yield against those for peak biomass (Fig. 10; $R^2 = 0.8946$) shows that for only 6 out of 52 parameters, the sensitivity indices lead to different classifications (e.g. important for yield, neither for peak biomass), and in only three cases are the classifications opposite (e.g. important for yield but unimportant for peak biomass), indicating biomass and yield are generally correlated. This agrees with previous findings from field trials (Sinclair *et al.* 1990).

Finally, we considered the evolution of the sensitivity indices for LAI, aboveground biomass and yield over time (Supporting Information–Supplementary Material S3), and used collinearity analysis (following De Swaef *et al.* (2019); Coudron *et al.* (2021)) to assess identifiability of the model. The collinearity index used here was proposed by Brun *et al.* (2001) as a measure of linear dependencies between model parameters. Our results show that the model is generally identifiable (Figs. S4 and S5), with all collinearity values for LAI and biomass (and most for yield) below the commonly used threshold of 20, and the majority of values for all three outputs below the stricter threshold of 15.

6. DISCUSSION

Over recent decades, many modellers have developed functional-structural plant models to gain understanding of plant development. However, as these models become more detailed, they typically involve huge parameter sets, making it challenging to explore the parameter space and infer how the choice of parameters influences model predictions. Furthermore, the size of the parameter space makes it impractical to identify optimal parameter regions that would be predicted to maximise

outputs like light capture, biomass production or grain production. Modelling studies are therefore typically limited to using a defined parameter set and exploring the influence of a handful of plant traits. A notable exception is found in Rangarajan *et al.* (2022), who performed multi-objective optimization on an FSP model to identify optimal root phenotypes.

Whenever models use parameter values estimated from the experimental literature, it is often unclear whether any errors in measurement or differences between species would influence model predictions and where more detailed measurements would be beneficial.

To address these challenges, we have explored the use of global sensitivity analysis (GSA), which identifies important (and unimportant) parameters for a given model output. Our study has demonstrated that GSA provides useful insights both for our biological understanding of plant development and for guiding further model development and parameterization.

Modelling insights In terms of model development, GSA enables us to identify unimportant parameters, so that they may be set to a fixed value, thereby decreasing dimensionality of the typically large model parameter space. Efforts can then be concentrated on accurately estimating the most important input parameters. In addition, identifying the most important parameters can significantly ease the task of finding the optimal set of plant characteristics for a given trait.

Out of 52 input parameters, only 12 were identified as important for yield and peak biomass (14 for LAI), while over 70 % of inputs were deemed unimportant (Fig. 4). This highlights the benefit of incorporating GSA in the modelling process, as it suggests a rough estimate suffices for the majority of

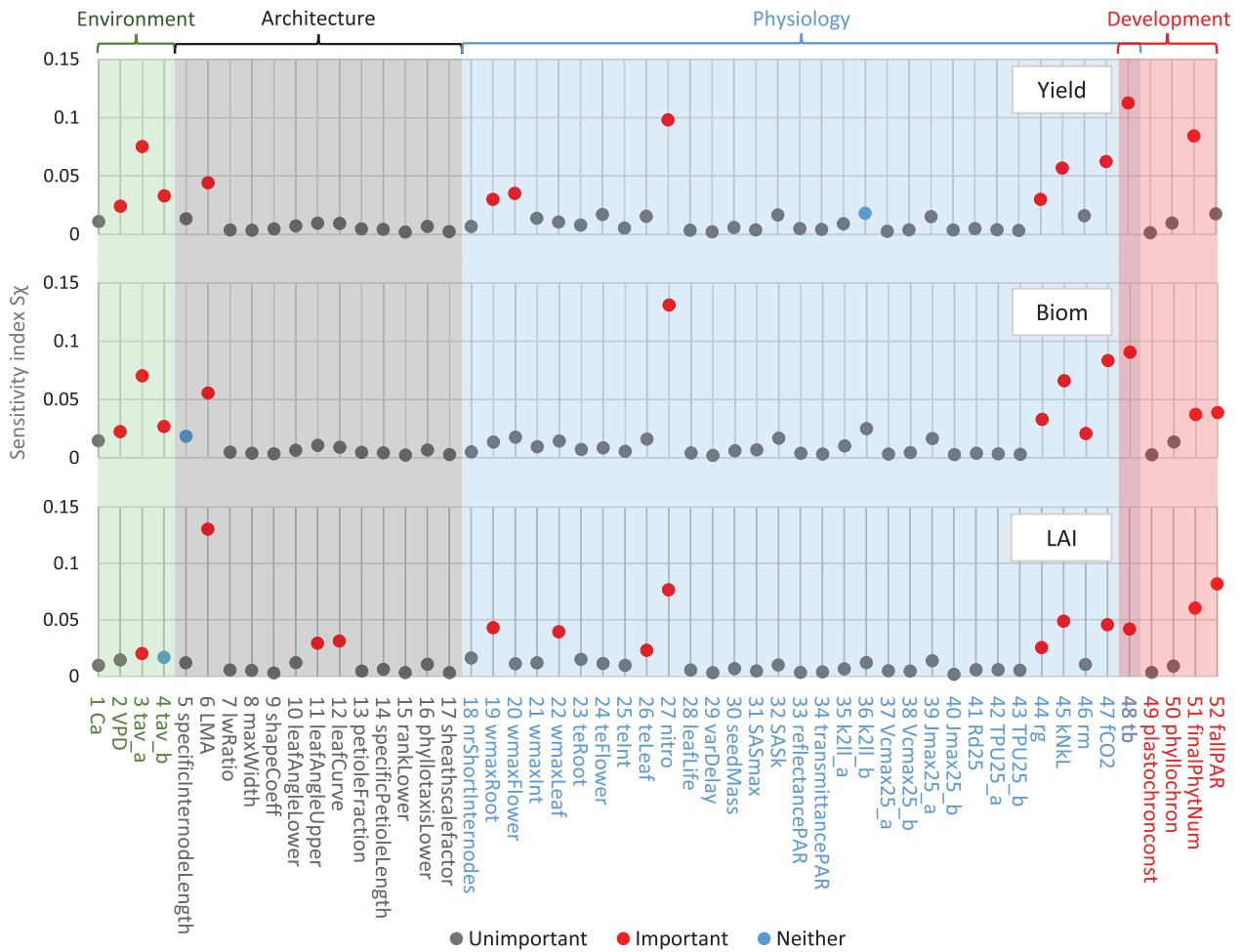


Figure 4. Sensitivity indices $S_{\chi}(i, j)$ Equation (8) for different outputs. See Table 1 for more information about the input parameters.

input parameter values. Our analysis revealed that the important parameters included leaf nitrogen content (parameter 27: nitro), base temperature (parameter 48: tb), conversion factor of CO_2 to biomass (parameter 47: fCO₂) and leaf mass per unit area (parameter 6: LMA). Interestingly, some of the important parameters cannot generally be measured in an experimental setting, or at best can only be roughly estimated. Among these are theoretical maximum biomass of the root system, flower and leaf (parameters 19: wmaxRoot, 20: wmaxFlower and 22: wmaxLeaf).

The FvCB photosynthesis model is calibrated fairly precisely for C3 species, but as Yin and Struik (2009) note, several parameter estimates in the C4-equivalent contain more uncertainty. None of the FvCB parameters taken into account (parameters 35–43) are classified as important in our analysis, which suggests the C4 model can be reliably used with the values proposed in Yin and Struik (2009).

Some inputs identified as unimportant due to their low sensitivity index have a relatively high standard deviation of effects (Fig. 5, e.g., parameters 33: reflectancePAR; 34: transmittancePAR; 37: Vcmax25_a), with high fluctuations around a low mean, which could indicate non-linearity or interaction effects.

To quantify the importance of these fluctuations there is no one rule that fits all, but instead one should investigate those parameters with low sensitivity indices but high RSD further on an ad hoc basis as described in Section . Expert knowledge of the biological processes or model equations related to such inputs can help identify likely interaction effects and quantify their importance.

Most parameters related to crop architecture were classified as unimportant. This does not mean that architecture itself is not relevant. If a model does not address aspects of architecture, questions that rely on architecture cannot be addressed. As changes in architectural parameters (e.g. leaf length/width ratio or phyllotaxis) do lead to noticeable changes in plant architecture, we hypothesize this is due to the choice of outputs (yield, aboveground biomass and LAI), which are crop-level outputs. As a result, many parameters that are routinely deemed to be important in conventional crop models are also identified as important in our analysis. Considering specific structural outputs (e.g. average leaf area, number of leaves) might result in more architectural parameters being classified as important. Additionally, architectural parameters might play a bigger role in polycultures, whereas here a monoculture was simulated.

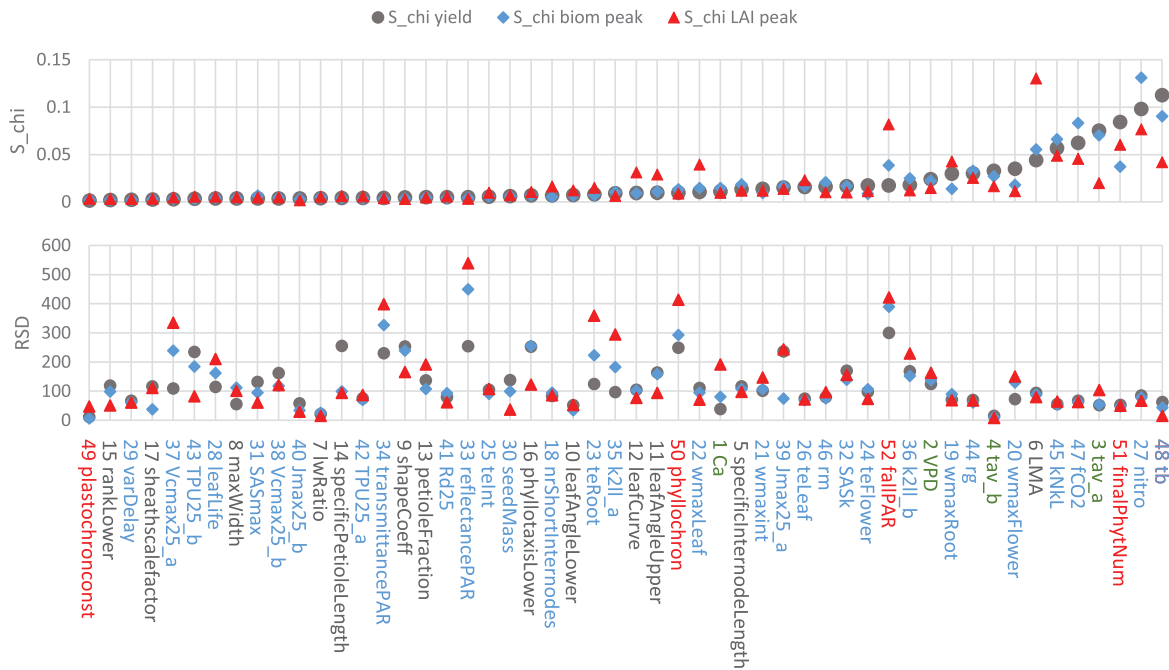


Figure 5. Sensitivity index S_{χ} Equation (8) and RSD Equation (14) for the three outputs ordered to the S_{χ} for yield. The label colours represent the parameter categories. Black: architectural; red: developmental; green: environmental; blue: physiological.

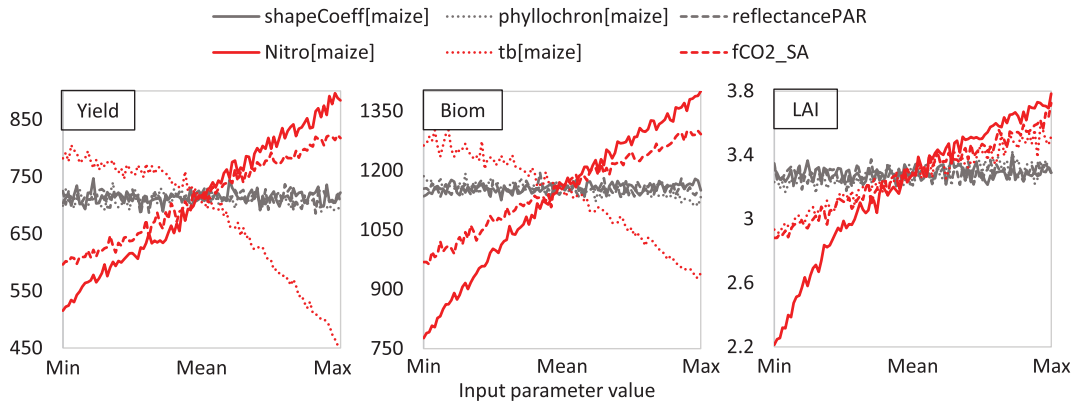


Figure 6. OAT simulations of 3 important parameters (red) and 3 unimportant parameters (grey). Each parameter is uniformly varied over its input range (Table 1), while the other parameters are set to the mean of their input ranges.

More generally, sensitivity results may change under different scenarios (e.g. management or environmental) (Richter *et al.* 2010; Coudron *et al.* 2021). Architectural parameters might for example become more important with increased competition (higher plant densities) or with increased variability in plant traits (e.g. intercropping several maize varieties). Sensitivity indices may also change over time. In our analysis, this was the case for the output peak aboveground biomass (see Fig. S3), where parameters related to initial development (e.g. parameter 30: seed mass) were initially important, but became less relevant at later points in time, while, for example, parameter 27: leaf nitrogen content became more important over time.

One should, therefore, carefully consider the applicability and generalizability of sensitivity results.

Biological insights We expect several conclusions to extend to different crop species, crop designs or environmental conditions within this model. Parameters that are part of major conserved mechanisms, such as photosynthesis and growth, are likely to be equally insensitive independent of the species or conditions (within biologically sensible ranges). For stress events like drought or heat, GSA specific for such conditions would need to be done. Interestingly, we found that several architectural parameters were unimportant for model output, in contrast to some model-aided trait analyses for other species that do show

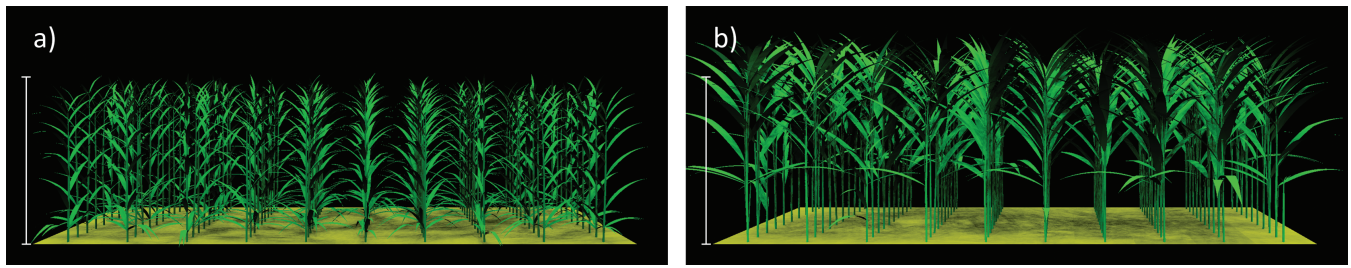


Figure 7. Architectural differences in a stand of maize caused by a difference in leaf nitrogen content (parameter 27) (identified as an important parameter) at the end of simulation day 99. The other parameters are set to the mean of their input ranges (Table 1). (A) nitro = 1.5 g m^{-2} ; lower bound of input range. Yield = 516 g m^{-2} , peak biomass = 777 g m^{-2} , peak LAI = 2.2. (B) nitro = 4 g m^{-2} ; upper bound of input range. Yield = 884 g m^{-2} , peak biomass = 1401 g m^{-2} , peak LAI = 3.8. See also Fig. 6.

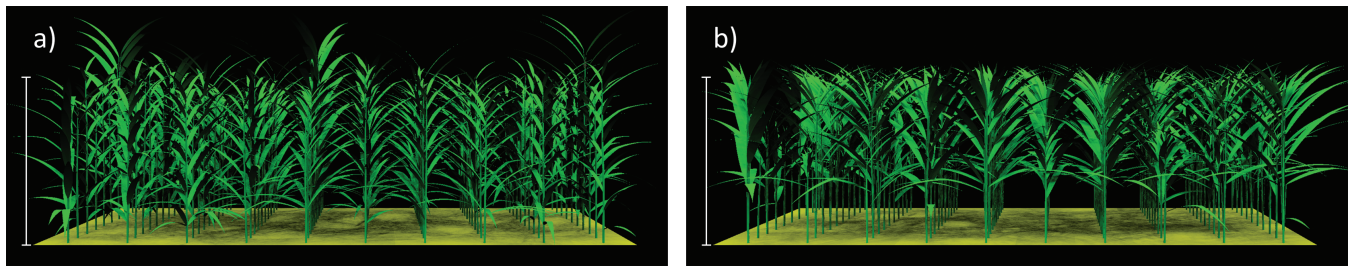


Figure 8. Architectural differences in a stand of maize caused by a difference in phyllochron (parameter 50) (identified as an unimportant parameter) at the end of simulation day 99. The other parameters are set to the mean of their input ranges (Table 1). (A) Phyllochron = 25 °C day ; lower bound of input range. Yield = 700 g m^{-2} , peak biomass = 1185 g m^{-2} , peak LAI = 3.2. (B) Phyllochron = 35 °C day ; upper bound of input range. Yield = 700 g m^{-2} , peak biomass = 1133 g m^{-2} , peak LAI = 3.3. Despite these architectural differences, the model outputs shown here and in Fig. 6 show that phyllochron is not important for yield, peak biomass or peak LAI.

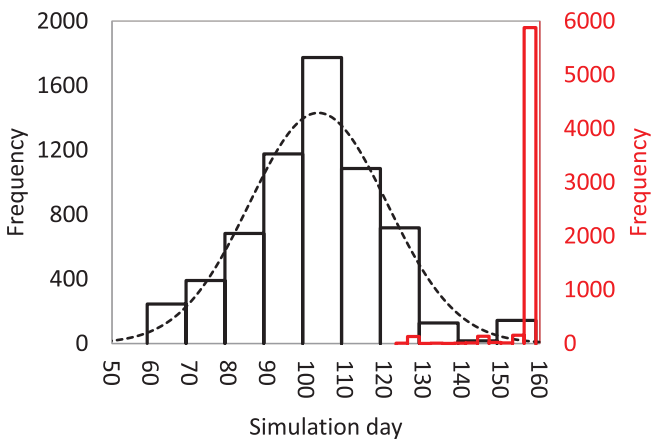


Figure 9. Histogram of the simulation day when peak LAI (black; primary vertical axis) and peak biomass (red; secondary vertical axis) are achieved. The right-most box contains simulations where the maximum was achieved at the final simulation day, so likely the majority of those would have reached their global maximum after that day.

the relevance of architectural parameters (Sarlikioti et al. 2011; Barillot et al. 2014; Zhu et al. 2015; Li et al. 2021). This discrepancy might have been caused by the difference in the output under consideration. We focused on LAI, biomass growth and

yield, whereas the studies cited analysed the effect of architectural traits on light capture and photosynthesis without feedback on plant growth.

Parameters governing shade avoidance response were identified as unimportant. This is not surprising, since the relatively uniform maize canopy we simulated leads to approximately the same response in all plants. This would likely be different in more heterogeneous mixed-species stands where performance depends on plastic plant responses to local conditions (Zhu et al. 2015).

Leaf appearance rate (phyllochron) is known to have a significant impact on plant architecture, is typically deemed as an important parameter in crop models, and has received significant interest as a potential breeding target to bring forward the flowering date (Wilhelm and McMaster 1995; Birch et al. 1998; Padilla and Otegui 2005; Clerget et al. 2008; dos Santos et al. 2022). Interestingly, phyllochron was classified as unimportant in our study. Variations in phyllochron—as expected—did lead to visible changes in plant architecture (Fig. 8). However, these architectural changes did not lead to significant changes in field-level outputs yield, biomass or LAI. We hypothesize that the expected increase in total leaf area as a result of lower phyllochron is counteracted by increased competition between the higher number of leaves. This leads to a near-constant peak LAI, which subsequently does not lead to significant changes in peak biomass and yield.

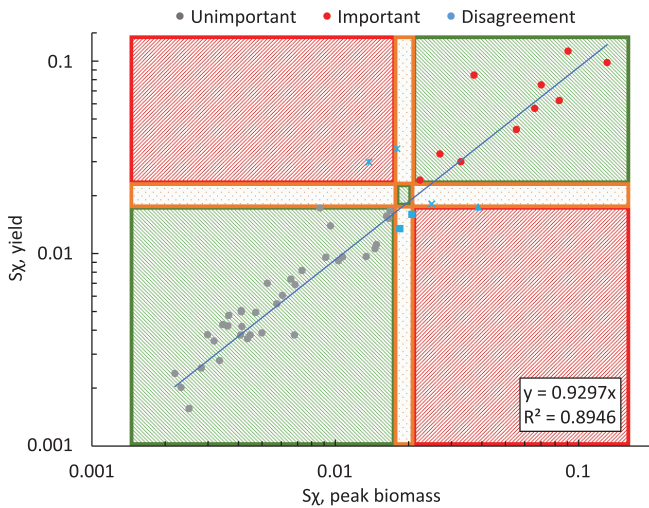


Figure 10. Peak biomass as proxy for yield, with indications of which sensitivity indices agree and which do not. Green area (diagonal lines top-left to bottom-right): indices agree; orange area (dotted): input (un)important for one output, neither for the other; red area (diagonal lines bottom-left to top-right): input important for one output, unimportant for the other. Markers: grey: parameter unimportant for both outputs; red: important for both outputs; blue: disagreeing classifications for different output.

To conclude, this work shows that including global sensitivity analysis in the modelling routine for FSP models can lead to a variety of insights about both the model and the biological processes it describes. GSA is applicable to any model, and should therefore become a standard consideration for any FSP modeller. However, as sensitivity results may change under different scenarios or models, the applicability and generalizability of sensitivity results should be inferred with caution.

SUPPORTING INFORMATION

- S1. Trajectory generation
- S2. Input parameters with fixed values
- S3. Exploratory data analysis
- S4. Effects for three unimportant inputs with high RSD

They contain the following:

- S1: Detailed information on the used trajectory generation method for our Elementary Effects analysis
- S2: Table of parameter values used in EE analysis
- S3: Additional figures showing results from EE analysis
- S4: Figure of effects for three unimportant inputs with high relative standard deviation

ACKNOWLEDGMENTS

This work was supported by the University of Nottingham Future Food Beacon of Excellence. We gratefully acknowledge the constructive feedback provided by two anonymous reviewers.

CONFLICT OF INTEREST STATEMENT

None declared.

DATA AVAILABILITY

The numerical results were obtained using code in the RGG language [Kniemeyer \(2008\)](#) (an extension of Java), compiled on the freely available modelling environment GroIMP [Hemmerling et al. \(2008\)](#). Included in the code is a stand-alone implementation of our formulation of EE. The data are available in the form of Microsoft Excel spreadsheets. All code and data that support the findings of this study are openly available at https://github.com/pmxxr3/EE_applied_2023 and as [Supporting Information—supplementary materials](#) to this paper.

LITERATURE CITED

- Bailey B.N., Kent E.R. 2021. On the resolution requirements for accurately representing interactions between plant canopy structure and function in three-dimensional leaf-resolving models. *in silico Plants* 3(2):diab023.
- Barillot, R., Escobar-Gutiérrez, A.J., Fournier, C., Huynh, P. and Combes, D. 2014. Assessing the effects of architectural variations on light partitioning within virtual wheat-pea mixtures. *Annals of Botany* 114(4):725–737.
- Birch, C.J., Vos, J., Kiniry, J., Bos, H.J. and Elings, A. 1998. Phyllochron responds to acclimation to temperature and irradiance in maize. *Field Crops Research* 59(3):187–200.
- Brun R., Reichert, P. and Künsch, H.R. 2001. Practical identifiability analysis of large environmental simulation models. *Water Resources Research* 37(4):1015–1030.
- Buck-Sorlin, G., de Visser, P.H., Henke, M., Sarlikioti, V., van Der Heijden, G.W., Marcelis, L.F. and Vos, J. 2011. Towards a functional-structural plant model of cut-rose: simulation of light environment, light absorption, photosynthesis and interference with the plant structure. *Annals of Botany* 108(6):1121–1134.
- Box G.E.P., Meyer R.D. 1986. An analysis for unreplicated fractional factorials. *Technometrics* 28(1):11–18.
- Campolongo, F., Saltelli, A. and Cariboni, J. 2011. From screening to quantitative sensitivity analysis: a unified approach. *Computer Physics Communications* 182(4):978–988.
- Casadebaig, P., Zheng, B., Chapman, S., Huth, N., Faivre, R. and Chenu, K. 2016. Assessment of the potential impacts of wheat plant traits across environments by combining crop modeling and global sensitivity analysis. *PLOS ONE* 11(1):1–27.
- Caubel, J., Launay, M., Ripoche, D., Gouache, D., Buis, S., Huard, F., Huber, L., Brun, F. and Bancal, M.O. 2017. Climate change effects on leaf rust of wheat: implementing a coupled crop-disease model in a French regional application. *European Journal of Agronomy* 90:53–66.
- Clerget, B., Dingkuhn, M., Gozé, E., Rattunde, H.F.W. and Ney, B. 2008. Variability of phyllochron, plastochron and rate of increase in height in photoperiod-sensitive sorghum varieties. *Annals of Botany* 101(4):579–594.
- Coudron, W., Gobin, A., Boeckert, C., De Cuyper, T., Lootens, P., Pollet, S., Verheyen, K., De Frenne, P. and De Swaef, T. 2021. Data collection design for calibration of crop models using practical identifiability analysis. *Computers and Electronics in Agriculture* 190:106457.
- Cournède, P.H., Chen, Y., Wu, Q., Baey, C. and Bayol, B. 2013. Development and evaluation of plant growth models: methodology and implementation in the PYGMALION platform. *Mathematical Modelling of Natural Phenomena* 8(4):112–130.

- Coussement, J.R., De Swaef, T., Lootens, P., Roldán-Ruiz, I. and Steppe, K. 2018. Introducing turgor-driven growth dynamics into functional-structural plant models. *Annals of Botany* 121(5):849–861.
- De Swaef, T., Bellocchi, G., Aper, J., Lootens, P. and Roldán-Ruiz, I. 2019. Use of identifiability analysis in designing phenotyping experiments for modelling forage production and quality. *Journal of Experimental Botany* 70(9):2587–2604.
- De Vries, J., Evers, J.B., Poelman, E.H. and Anten, N.P. 2020. Optimal plant defence under competition for light and nutrients: an evolutionary modelling approach. *in silico Plants* 2(1):diaa008.
- Dubois, J.J.B., Fiscus, E.L., Booker, F.L., Flowers, M.D. and Reid, C.D. 2007. Optimizing the statistical estimation of the parameters of the Farquhar–von Caemmerer–Berry model of photosynthesis. *New Phytologist* 176(2):402–414.
- Dos Santos, C.L., Abendroth, L.J., Coulter, J.A., Nafziger, E.D., Suyker, A., Yu, J., Schnable, P.S. and Archontoulis, S.V. 2022. Maize leaf appearance rates: a synthesis from the United States corn belt. *Frontiers in Plant Science* 13:872738.
- Evers J.B., Bastiaans L. 2016. Quantifying the effect of crop spatial arrangement on weed suppression using functional-structural plant modelling. *Journal of Plant Research* 129(3):339–351.
- Gauthier, M., Barillot, R. and Andrieu, B. 2021. Simulating grass phenotypic plasticity as an emergent property of growth zone responses to carbon and nitrogen metabolites. *in silico Plants* 3(2):diab034.
- Goudriaan J., Van Laar H.H. 1994. *Modelling potential crop growth processes*. Vol. 2. Dordrecht: Kluwer Academic Publishers.
- Hemmerling, R., Kniemeyer, O., Lanwert, D., Kurth, W. and Buck-Sorlin, G.H. 2008. The rule-based language XL and the modelling environment GroIMP illustrated with simulated tree competition. *Functional Plant Biology* 35:9–10.
- Henke, M., Kurth, W. and Buck-Sorlin, G.H. 2016. FSPM-P: towards a general functional-structural plant model for robust and comprehensive model development. *Frontiers of Computer Science* 10(6):1103–1117.
- Heuvelink. 1996. Re-interpretation of an experiment on the role of assimilated transport resistance in partitioning in tomato. *Annals of Botany* 78(4):467–470.
- Hickernell F.J. 2000. *What affects the accuracy of quasi-Monte Carlo quadrature?*. Berlin, Heidelberg, Germany: Springer, 16–55.
- Huber, M., Nieuwendijk, N.M., Pantazopoulou, C.K. and Pierik, R. 2021. Light signalling shapes plant–plant interactions in dense canopies. *Plant, Cell & Environment* 44(4):1014–1029.
- Iooss B. et al. 2021. *sensitivity: global Sensitivity Analysis of Model Outputs*. R package version 1.27.0.
- Kniemeyer O. 2008. *Design and implementation of a graph grammar based language for functional-structural plant modelling*. BTU Cottbus-Senftenberg, Germany: Doctoral Thesis.
- Li, S., van Der Werf, W., Zhu, J., Guo, Y., Li, B., Ma, Y. and Evers, J.B. 2021. Estimating the contribution of plant traits to light partitioning in simultaneous maize/soybean intercropping. *Journal of Experimental Botany* 72(10):3630–3646.
- Mathieu, A., Vidal, T., Jullien, A., Wu, Q. and Cournède, P.H. 2016. Sensitivity analysis to help individual plant model parameterization for winter oilseed rape. *2016 IEEE International Conference on Functional-Structural Plant Growth Modeling, Simulation, Visualization and Applications (FSPMA)*, 133–139.
- Menberg, K., Heo, Y. and Choudhary, R. 2016. Sensitivity analysis methods for building energy models: comparing computational costs and extractable information. *Energy and Buildings* 133:433–445.
- Morris M.D. 1991. Factorial sampling plans for preliminary computational experiments. *Technometrics* 33(2):161–174.
- Morokoff W.J., Caflich R.E. 1994. Quasi-random sequences and their discrepancies. *SIAM Journal on Scientific Computing* 15(6):1251–1279.
- Owen A.B. 2014. Sobol’ indices and Shapley value. *SIAM/ASA Journal on Uncertainty Quantification* 2(1):245–251.
- Pao, Y.C., Kahlen, K., Chen, T.W., Wiechers, D. and Stützel, H. 2021. How does structure matter? Comparison of canopy photosynthesis using one- and three-dimensional light models: a case study using greenhouse cucumber canopies. *in silico Plants* 3(2):diab031.
- Pianosi, F., Sarrazin, F. and Wagener, T. 2015. A Matlab toolbox for global sensitivity analysis. *Environmental Modelling & Software* 70:80–85.
- Pianosi, F., Beven, K., Freer, J., Hall, J.W., Rougier, J., Stephenson, D.B. and Wagener, T. 2016. Sensitivity analysis of environmental models: a systematic review with practical workflow. *Environmental Modelling and Software* 79:214–232.
- Puy, A., Lo Piano, S. and Saltelli, A. 2021. Is VARS more intuitive and efficient than Sobol’ indices? *Environmental Modelling and Software* 137:104960.
- Padilla J.M., Otegui M.E. 2005. Coordination between leaf initiation and leaf appearance in field-grown maize (*Zea mays*): genotypic differences in response of rates to temperature. *Annals of Botany* 96(6):997–1007.
- Qian G., Mahdi A. 2020. Sensitivity analysis methods in the biomedical sciences. *Mathematical Biosciences* 323:108306.
- Rangarajan, H., Hadka, D., Reed, P. and Lynch, J.P. 2022. Multi-objective optimization of root phenotypes for nutrient capture using evolutionary algorithms. *The Plant Journal* 111(1):38–53.
- Razavi S., Gupta H.V. 2015. What do we mean by sensitivity analysis? The need for comprehensive characterization of ‘global’ sensitivity in Earth and Environmental systems models. *Water Resources Research* 51(5):3070–3092.
- Razavi, S., Jakeman, A., Saltelli, A., Prieur, C., Iooss, B., Borgonovo, E., Plischke, E., Piano, S.L., Iwanaga, T., Becker, W. and Tarantola, S. 2021. The future of sensitivity analysis: an essential discipline for systems modeling and policy support. *Environmental Modelling and Software* 137:104954.
- Richter, G.M., Acutis, M., Trevisiol, P., Latiri, K. and Confalonieri, R. 2010. Sensitivity analysis for a complex crop model applied to Durum wheat in the Mediterranean. *European Journal of Agronomy* 32(2):127–136.
- Ruano, M.V., Ribes, J., Seco, A. and Ferrer, J. 2012. An improved sampling strategy based on trajectory design for application of the Morris method to systems with many input factors. *Environmental Modelling and Software* 37:103–109.
- Rutjens, R.J., Band, L.R., Jones, M.D. and Owen, M.R. 2023. Elementary effects for models with dimensional inputs of arbitrary type and range: scaling and trajectory generation. *Plos ONE* 18(10):e0293344.
- Roberts M. 2021. The unreasonable effectiveness of quasirandom sequences. <http://extremelearning.com.au/unreasonable-protect-penalty-z@effectiveness-of-quasirandom-sequences/>. (02 July 2021).
- Sainte-Marie J., Cournède P.-H. 2019. Insights of global sensitivity analysis in biological models with dependent parameters. *Journal of Agricultural, Biological and Environmental Statistics* 24(1):92–111.
- Saltelli A., Annoni P. 2010. How to avoid a perfunctory sensitivity analysis. *Environmental Modelling and Software* 25(12): 1508–1517.
- Saltelli A., Tarantola S. 2002. On the relative importance of input factors in mathematical models. *Journal of the American Statistical Association* 97(459):702–709.
- Saltelli, A., Ratto, M., Andres, T., Campolongo, F., Cariboni, J., Gatelli, D., Saisana, M. and Tarantola, S. 2008. *Global sensitivity analysis: the primer*. Chichester, England: John Wiley & Sons.
- Saltelli, A., Annoni, P., Azzini, I., Campolongo, F., Ratto, M. and Tarantola, S. 2010. Variance based sensitivity analysis of model output: design and estimator for the total sensitivity index. *Computer Physics Communications* 181(2):259–270.
- Sarlikioti, V., de Visser, P.H., Buck-Sorlin, G.H. and Marcelis, L.F.M. 2011. How plant architecture affects light absorption and photosynthesis in tomato: towards an ideotype for plant architecture using a functional–structural plant model. *Annals of Botany* 108(6):1065–1073.

- Silvestro, P.C., Pignatti, S., Yang, H., Yang, G., Pascucci, S., Castaldi, F. and Casa, R. 2017. Sensitivity analysis of the Aquacrop and SAFYE crop models for the assessment of water limited winter wheat yield in regional scale applications. *PLOS ONE* 12(11):1–30:e0187485.
- Sinclair, T.R., Bennett, J.M. and Muchow, R.C. Relative sensitivity of grain yield and biomass accumulation to drought in field-grown maize. *Crop Science* 30(3):crops1990.0011183X003000030043x.
- Spitters, C.J.T., Toussaint, H.A.J.M. and Goudriaan, J. 1986. Separating the diffuse and direct component of global radiation and its implications for modeling canopy photosynthesis. Part I. Components of incoming radiation. *Agricultural and Forest Meteorology* 38(1):217–229.
- Spitters C.J.T. 1986. Separating the diffuse and direct component of global radiation and its implications for modeling canopy photosynthesis. Part II. Calculation of canopy photosynthesis. *Agricultural and Forest Meteorology* 38(1):231–242.
- Streit, K., Henke, M., Bayol, B., Cournède, P.H., Sievänen, R. and Kurth, W. 2016. Impact of geometrical traits on light interception in conifers: analysis using an FSPM for Scots pine. 2016 *IEEE International Conference on Functional-Structural Plant Growth Modeling, Simulation, Visualization and Applications (FSPMA)*, 194–203.
- Uys, L., Hofmeyr, J.H.S. and Rohwer, J.M. 2021. Coupling kinetic models and advection–diffusion equations. 2. Sensitivity analysis of an advection–diffusion–reaction model. *in silico Plants* 3(1):diab014.
- Van Der Meer, M., De Visser, P.H., Heuvelink, E. and Marcelis, L.F. 2021. Row orientation affects the uniformity of light absorption, but hardly affects crop photosynthesis in hedgerow tomato crops. *in silico Plants* 3(2):diab025.
- Vanuytrecht, E., Raes, D. and Willems, P. 2014. Global sensitivity analysis of yield output from the water productivity model. *Environmental Modelling & Software* 51:323–332.
- Vos, J., Marcelis, L.F.M., & Evers, J.B. 2007. Functional-structural plant modelling in crop production. In *Functional-structural plant modelling in crop production*. Dordrecht: Springer, 1–12.
- Yang Z., Becerik-Gerber B. 2015. A model calibration framework for simultaneous multi-level building energy simulation. *Applied Energy* 149:415–431.
- Yin X., Struik P.C. 2009. C3 and C4 photosynthesis models: an overview from the perspective of crop modelling. *NJAS - Wageningen Journal of Life Sciences* 57(1):27–38.
- Yin, X., Goudriaan, J.A.N., Lantinga, E.A., Vos, J.A.N. and Spiertz, H.J. 2003. A flexible sigmoid function of determinate growth. *Annals of Botany* 91(3):361–371.
- Wilhelm W.W., McMaster G.S. 1995. Importance of the phyllochron in studying development and growth in grasses. *Crop Science* 35(1):crops1995.0011183X003500010001x.
- Wu J. 2020. A new sequential space-filling sampling strategy for elementary effects-based screening method. *Applied Mathematical Modelling* 83:419–437.
- Zhou, H., Zhou, G., He, Q., Zhou, L., Ji, Y. and Zhou, M. 2020. Environmental explanation of maize specific leaf area under varying water stress regimes. *Environmental and Experimental Botany* 171:103932.
- Zhu, J., van der Werf, W., Anten, N.P., Vos, J. and Evers, J.B. 2015. The contribution of phenotypic plasticity to complementary light capture in plant mixtures. *New Phytologist* 207(4):1213–1222.
- Zhu, J., Dai, Z., Vivin, P., Gambetta, G.A., Henke, M., Peccoux, A., Ollat, N. and Delrot, S. 2017. A 3-D functional–structural grapevine model that couples the dynamics of water transport with leaf gas exchange. *Annals of Botany* 121(5):833–848.
- Zhu, J., Gou, F., Rossouw, G., Begum, F., Henke, M., Johnson, E., Holzapfel, B., Field, S. and Seleznyova, A. 2021. Simulating organ biomass variability and carbohydrate distribution in perennial fruit crops: a comparison between the common assimilate pool and phloem carbohydrate transport models. *in silico Plants* 3(2):diab024.